Chemical Engineering and Processing 82 (2014) 123–131

Contents lists available at ScienceDirect

Chemical Engineering and Processing: Process Intensification

journal homepage: www.elsevier.com/locate/cep

Intensification of convective heat transfer in water/ethylene glycol based nanofluids containing TiO_2 nanoparticles

B.A. Bhanvase[a,*], M.R. Sarode[c], L.A. Putterwar[c], Abdullah K.A.[c], M.P. Deosarkar[c], S.H. Sonawane[b]

[a] Department of Chemical Engineering, Laxminarayan Institute of Technology, Amaravati Road, Nagpur 440033, India
[b] Department of Chemical Engineering, National Institute of Technology, Warangal AP 506004 India
[c] Department of Chemical Engineering, Vishwakarma Institute of Technology, 666, Upper Indira Nagar, Pune 411 037, India

ARTICLE INFO

Article history:
Received 27 December 2013
Received in revised form 13 May 2014
Accepted 17 June 2014
Available online 24 June 2014

Keywords:
Nanofluid
Nusselt
Convective
Reynolds
TiO_2

ABSTRACT

This paper presents a study of heat transfer performance of water, ethylene glycol (EG) and their mixtures of varying compositions and comparison thereof. The present work demonstrates the enhancement in convective heat transfer in nanofluids. The nanofluids were prepared by adding TiO_2 nanoparticles (having a particle size below 100 nm) in a base fluid. A binary mixture of EG (40%) and water (60%) was used as a base fluid. Nanofluids with varied volume fraction between 0 and 0.5 (volume fraction of TiO_2 nanoparticles) were considered in the present study. The experimental setup used was consisting of a test section that includes 750 mm long copper pipe with 8 mm inner diameter and a heater. The test section was covered with an insulation layer to minimize the heat losses. Temperature measurement was done with thermocouples. The experiments were conducted to study the effects of solid volume fraction, nanofluid flow rate and the inlet temperature on the heat transfer performance of the nanofluids. The results show an enhancement in heat transfer coefficient with increased volume fraction of TiO_2 nanoparticles. The maximum enhancement of 105% in heat transfer coefficient was observed for the nanofluid with solid volume fraction of 0.5.

1. Introduction

The notion of the addition of nanofluids to effect enhancement in heat transfer [1–3], and mass transfer [4,5], was initially proposed by Choi [1]. There after this application has gained significant attention in the study of heat transfer phenomena. The nanofluids have found their applications in a number of industries. These applications include transportation, power generation, micro-manufacturing, chemical and metallurgical industries, as well as heating, cooling, ventilation and air-conditioning industry. Such applications become important due to alteration in the properties of the fluids such as thermal conductivity, viscosity etc. The industrial applications of nanofluids have gained importance because of some specific potential benefits such as improved heat transfer and stability, reduced pumping power, minimal clogging, miniaturized systems, and cost and energy savings [6–10].

Most conventional heat transfer fluids, such as water, ethylene glycol and engine oils have limited capabilities in terms of their thermal properties such as thermal conductivity, thermal diffusivity etc., which in turn, may impose severe restrictions in many thermal applications. The significant heat transfer enhancement by using liquid–solid particle mixture has been reported by earlier researchers [8–16]. Such enhancement is attributed to the increase in the fluid's effective thermal conductivity by the addition of solid particles [17–24]. However, the mixtures containing millimeter or micrometer size particles lead to serious problems to flow characteristics [25]. The reasons for these problems are a drastic increase in pressure drop and severe clogging that result due to rapid settling of particles of larger (micron) size. All of these difficulties will impose the severe limitations on effective heat transfer in different applications of liquid–solid mixtures. These problems can be effectively resolved by using nanofluids which consist of solid nanoparticles or nanofibers with sizes less than 100 nm suspended in liquid. The nanofluid is an agglomerate-free suspension of nanoparticles, which remains stable for longer time without causing any chemical changes in the base fluid. This is accomplished by (1) minimizing the density difference between solids and liquids,

* Corresponding author. Tel.: +91 712 2531659; fax: +91 712 2561107.
E-mail addresses: bharatbhanvase@gmail.com, bharatbhanvase@yahoo.com (B.A. Bhanvase).

http://dx.doi.org/10.1016/j.cep.2014.06.009
0255-2701/

Nomenclature

k	fluid thermal conductivity, W/m °C
x	axial distance from the inlet of the test section, m
h	convective heat transfer coefficient, W/m^2 °C
q_s	heat flux applied to the fluid, W/m^2
T_S	surface temperature, °C
T_b	fluid bulk temperature, °C
P	inner perimeter of the copper tube, m
$\dot{m}$	mass flow rate, kg/s
C_p	fluid specific heat, kJ/kg °C
A	inner surface area of the copper tube, m^2
D_i	inside diameter of copper tube, m
Nu	Nusselt number
V	fluid velocity, m/s
Pr	Prandtl number
Re	Reynolds number

Greek symbols

μ	fluid viscosity, Pa s
ρ	fluid density, kg/m^3
φ	particle volume fraction

Subscripts

p	particle
s	surface
b	bulk
i	inlet
o	outlet
f	fluid
bf	base fluid
nf	nanofluid
W	water
EG	ethylene glycol

(2) increasing the viscosity of the liquid, (3) using nanometer sized particles and (4) preventing particles from agglomeration.

The term nanofluid refers to a two-phase mixture that is composed of a continuous phase, and a dispersed phase made of extremely fine metallic/metal oxide particles (of size below 100 nm; and hence called as nanoparticles). The smaller size conducting solid particles will enhance the surface area per unit volume (aspect Ratio) due to a reduction in the size to nanometer, and thereby cause an increase in heat transfer performance. The addition of conducting nanoparticles to base fluids does enhance the heat transport by virtue of increase in the thermal conductivity and thermal diffusivity values of resulting nanofluid. Choi [1,16–18,26,27] was the first to employ the nanometer-sized particles in conventional fluids and showed a considerable increase in the nanofluid thermal conductivity. Further, several groups have shown enhancement in thermal conductivity with nanoparticles such as Al_2O_3, CuO etc. dispersed in water and EG based nanofluids [2,28–30]. The enhancement in thermal conductivity depends on several parameters such as type, size and shape of the nanoparticles, properties of the base fluid (like thermal conductivity, viscosity, specific heat, density etc.), presence of emulsifier, volume fraction of the nanomaterials, etc. The main limitations of using the base fluid alone are (1) a small range of working temperatures, and (2) low thermal conductivity. Peyghambarzadeh et al. [30] has reported that the combination of water and EG can overcome these limitations. The inherent problem with water to be used as heat transfer media is that it freezes at 0 °C or boils at 100 °C temperature, therefore it can not be used above 100 °C and below 0 °C temperature (i.e. freezing point and boiling point respectively). The working temperature range of the base fluid can be increased by using EG along with water due to anti-freezing properties of EG [31].

The heat transfer studies on nanofluids are divided into three groups: (1) estimation of the effective thermal conductivity under the static conditions, (2) evaluation of convective heat transfer performance and (3) heat transfer associated with the phase change. For forced convective heat transfer, Pak and Cho [25] have shown that the Nusselt number of Al_2O_3/water and TiO_2/water nanofluids increases with an increase in the volume fraction of suspended nanoparticles and the Reynolds number. They have used two metallic oxide particles, γ-alumina and titanium dioxide with mean diameters of 13 and 27 nm respectively. The range of the Reynolds and Prandtl numbers was $l0^4$–10^5 and 6.5–12.3, respectively. Further a new correlation (Eq. (1)) for the turbulent convective heat transfer has been proposed for the dilute dispersed fluids with submicron metallic oxide particles.

$$Nu = 0.021\, Re^{0.8} Pr^{0.5} \quad (1)$$

The thermal conductivity, viscosity and Cp was considered in Eq. (1) are of a diluted dispersed slurry. Similar observations have also been reported by Xie et al. [32] for graphite nanofluids in the laminar flow regime. He et al. [8] have reported heat transfer performance and flow behavior of TiO_2/water nanofluids flowing in an upward direction through a vertical pipe in both the laminar and turbulent flow regimes under a constant heat flux condition. The reported results showed the enhancement in the convective heat transfer coefficient with an increase in nanoparticle volume fraction in thee nanofluids in both the laminar and turbulent flow regimes for a given Reynolds number and particle size. Lee et al. [33] and Xuan and Li [34] have studied the heat transfer behavior in parallel channels using nanofluids. They reported a reduction in thermal resistance (1/thermal conductivity) by a factor of two in case of Al_2O_3/H_2O and Cu/water nanofluids respectively. Das et al. [35] have investigated nucleate pool boiling heat transfer of Al_2O_3/H_2O nanofluids using cylindrical cartridge heaters. The heat transfer performance was found decreased in the presence of nanoparticles in the nanofluid. Further it was reported that the decrease in the boiling performance is a strong function of tube diameter for narrow tubes. The decreased pool boiling heat transfer was also observed by Xuan and Li [34] for CuO/H_2O nanofluids.

The use of TiO_2 nanoparticles as conducting solids in the formulation of nanofluids is reported by several researchers [2,8,10,12,36–38] due to its advantages such as ease of availability, handling safety, higher heat transfer coefficients and excellent chemical and physical stability even without an additional stabilizer [8,10,36]. It is to be noted that the experimental investigations found in the literature are focused on the nanofluids with single basefluid and constant heat flux. However, the heat transfer of nanofluids with the use of combinations of basefluids has not been reported in the available literature. The present study is focussed on the investigation of the heat transfer enhancement of TiO_2/EG/water nanofluids for different basefluid concentrations (EG + water). Other parameters considered in experimental analysis are, the nanoparticle volume fraction, the Reynolds number and the inlet temperature. In the present study, the nanofluids were prepared by dispersing TiO_2 nanoparticles in the mixture of EG and water.

2. Experimental methods

2.1. Materials and nanofluids preparation

TiO_2 nanoparticles, ethylene glycol and deionized water were used for the preparation of nanofluids. TiO_2 nanoparticles of

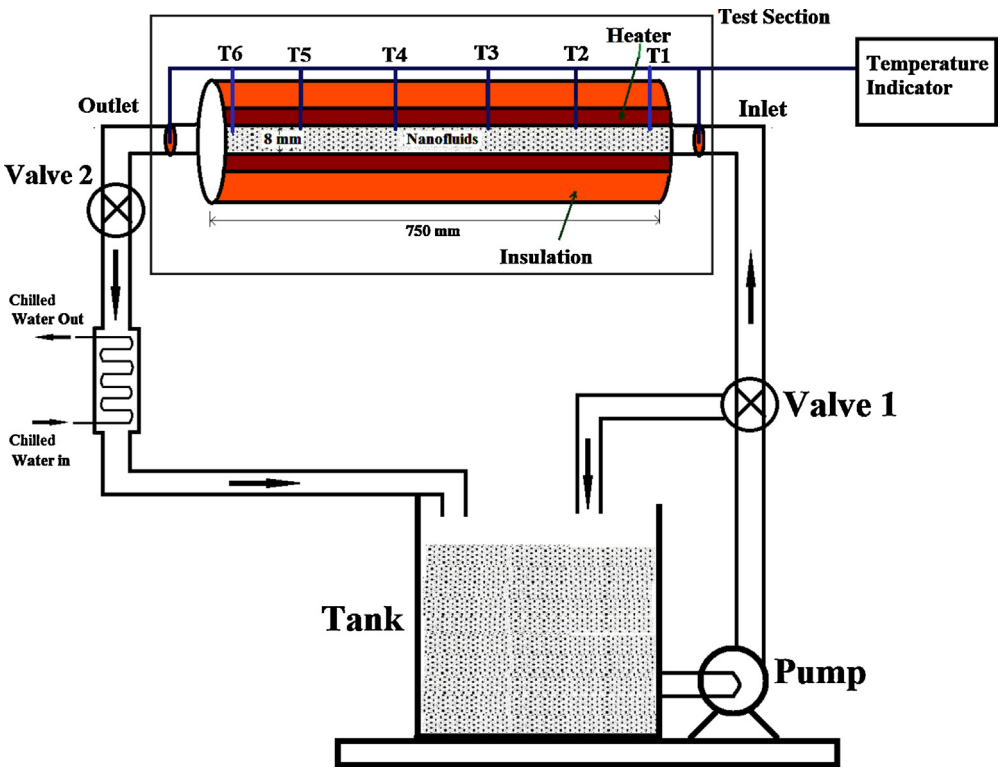

Fig. 1. Schematic of experimental setup for heat transfer enhancement studies using nanofluids.

particles size less than 100 nm have been used in this study. These TiO_2 nanoparticles were obtained from Kemphasol, Bombay. The X-ray diffraction analysis showed that the TiO_2 nanoparticles contain a dominantly rutile phase. Nanofluid samples were prepared by dispersing dry TiO_2 nanoparticles into EG–water mixture (basefluid). Further, after initial magnetic stirring for short duration, ultrasonication was effected and continued for about 30 min in order to obtain a uniform dispersion of TiO_2 nanoparticles in a basefluid [39]. Sodium dodecyl sulphate (SDS) procured from Merk Chemicals, Mumbai was used as dispersant; and it was added in 1:4 ratios with TiO_2 nanoparticle concentration. Ethylene glycol was obtained from Sigma Chemical Ind, Mumbai. Nanofluids containing 0.1–0.5% TiO_2 particles by volume were prepared as mentioned above.

2.2. Experimental set up and procedure for heat transfer coefficient measurements

The convective heat transfer characteristics of the nanofluid were studied using an indigenously fabricated set up. The schematic diagram of the experimental set up used to measure convective heat transfer coefficient is shown in Fig. 1. It consisted of a test section which includes 750 mm long copper pipe (ID 8 mm and OD 10 mm), heating coil, 8 mm thick insulation to avoid the heat losses and thermocouples. Also the temperature indicator, a power supply unit, a pump (Power: 0.5 HP, Monoblock 2800 RPM) and a condenser to maintain the required experimental conditions were used. The desired inlet temperature of nanofluid at the inlet of the test section was maintained by using the Julaboo cooling unit (REMI). The whole section was heated by a heating coil placed around the copper tube and connected to an adjustable AC power supply (0–230 V, 0–5 Amp). The experiments were carried out under constant heat flux conditions. Six thermocouples were mounted on the inner surface of the test section at axial positions located at and denoted as of 2.5 cm ($T_{S,1}$), 16.5 cm ($T_{S,2}$), 30.5 cm ($T_{S,3}$), 44.5 cm ($T_{S,4}$), 58.5 cm ($T_{S,5}$) and 72.5 cm ($T_{S,6}$) from the inlet of the test section, and were used to measure wall temperatures. Additionally, two thermocouples were mounted before and after the heat transfer section to measure the fluid bulk temperature at the inlet and outlet of the heat transfer section. All the thermocouples were calibrated prior to commencing experiments. The fluid was then passed through a heat exchanger and then through condenser to get required inlet temperature and recycled back to the storage tank. The pump was used with a bypass arrangement that was used to control the flow rate of the fluid. Three flow rates were selected such that the flow Reynolds number values were 900 (velocity = 0.48 m/s), 1200 (velocity = 0.63 m/s) and 1500 (velocity = 0.81 m/s). Steady state readings of temperatures and flow rates were measured during the experiments done for heat transfer analysis. These experiments were carried out to study the effect of volume fraction of nanoparticles, flow rates and the inlet temperature on heat transfer enhancement. Table 1 summarizes the experimental conditions those were used in this work.

Table 1
Operating conditions of the study.

Parameters	Nanofluid
Nanoparticles concentration (vol.%)	0.1–0.5
Reynolds number	900–1500
Flow type	Laminar
Inlet temperature	30–60 °C

2.3. Physical properties determination

It is well known that the determination of the nanofluids properties is a critical step in such type of experimental study. The thermal and physical properties of nanofluid can be calculated by using the correlations reported in the literature [26,32,33,40], which are given as follows:

$$Cp_{nf} = (1 - \varphi)Cp_{bf} + \varphi Cp_p \quad (2)$$

Table 2
Pure component thermo-physical properties at 30 °C [29,41].

Physical properties	Water	Ethylene glycol (EG)	TiO_2	Basefluid (40% EG)	Nanofluid (vol.%)				
					0.1	0.2	0.3	0.4	0.5
ρ (kg/m^3)	995.1	1088	4200	1032.26	1049.15	1052.31	1055.46	1058.62	1061.77
μ (Pa s)	0.0008	0.0141	–	0.0061	0.004402	0.004413	0.004424	0.004435	0.004447
k (W/m °C)	0.6194	0.2532	8.9538	0.4729	1.0026	1.0052	1.0077	1.0103	1.0129
Cp (J/kg °C)	4174	2430.8	4400	3476.72	3385.42	3386.43	3387.45	3388.46	3389.48
Pr	5.238	135.696	–	31.848	14.8644	14.8680	14.8717	14.8756	14.8796

$$\rho_{nf} = (1-\varphi)\rho_{bf} + \varphi\rho_p \quad (3)$$

where Cp_{nf} is specific heat capacity of nanofluids, Cp_{bf} specific heat capacity of basefluid, Cp_p specific heat capacity of nanoparticles, ρ_{nf} is density of nanofluids, ρ_{bf} density of basefluid, ρ_p density of nanoparticles, φ is nanoparticle volume fraction. The estimated physical properties of nanofluids were used in the correelation of Re, Pr and Nu.

The thermal conductivity of the TiO_2 nanoparticles is higher as compared to any combination of binary mixture of EG and water. Therefore, there is a remarkable increase in thermal conductivity of nanofluids when these nanoparticles are suspended in the basefluid. The thermal conductivity enhancement ratio is defined as the ratio of thermal conductivity of the nanofluid to that of the basefluid (k_{nf}/k_{bf}). Maxwell [41] proposed a model (Eq. (4)) to calculate the effective thermal conductivity of a two-phase mixture consisting of a continuous and dispersed phase.

$$k_{nf} = \frac{k_p + 2k_{bf} + 2\varphi(k_p - k_{bf})}{k_p + 2k_{bf} - \varphi(k_p - k_{bf})} k_{bf} \quad (4)$$

where k_p and k_{bf} are the thermal conductivities of the solid particles and the basefluid respectively, and φ is the solid volume fraction. Maxwell's model (Eq. (4)) is based on the assumptions that the solid particles are spherical in shape and the thermal conductivity of nanofluid depends on the thermal conductivities of solid particles and the basefluid and the particle volume fraction.

The effective viscosity of dilute suspensions containing spherical solid particles can be calculated by using the well-known Einstein's formula (Eq. (5)). Einstein's formula was found to be valid in cases dilute suspensions of relatively low solid volume fractions. For calculation of nanofluid viscosities, the following correlations were used:

$$\frac{\mu_{nf}}{\mu_{bf}} = 1 + 2.5\varphi \quad (5)$$

$$\mu_{bf} = (1-\varphi_{EG})\mu_W + \varphi_{EG}\mu_{EG} \quad (6)$$

where μ_{nf}, μ_{bf}, μ_W, and μ_{EG} are the viscosities of the nanofluids, basefluid, water and ethylene glycol respectively; φ_{EG} is the ethylene glycol volume fraction. The pure component properties of water, ethylene glycol and the basefluid are given in Table 2.

2.4. Convective heat transfer measurement

The convective heat transfer coefficient $h(x)$ at an axial distance 'x' from the inlet is defined as:

$$h(x) = \frac{q_s}{T_s(x) - T_b(x)} \quad (7)$$

where q_s heat flux applied to the fluid; while the wall temperature is being measured at a distance 'x' from the inlet, and that the fluid bulk temperature being measured at a distance 'x' from the inlet are $T_s(x)$ and $T_b(x)$ respectively. The bulk temperature of the fluid ($T_b(x)$) at an axial distance, x was estimated from the energy balance equation (Eq. (8)).

$$T_b(x) = T_{b,i} + \frac{q_s P}{\dot{m} \cdot C_p} \quad (8)$$

where $T_{b,i}$, P, x, $\dot{m}$ and C_p are bulk fluid temperature at the inlet, the perimeter of the copper tube, axial distance from the inlet of the test section, mass flow rate of the fluid, and specific heat capacity of the fluid, respectively. Further, in order to estimate the convective heat transfer coefficient, the amount of energy transferred to fluid is required to estimate from the inner surface area of the tube which is exposed to the nanofluid. The heat flux applied to the fluid can be estimated using the following equation (Eq. (9)).

$$q_s = \frac{\dot{m}\, C_p (T_{b,o} - T_{b,i})}{A} \quad (9)$$

where, $T_{b,o}$, $T_{b.i}$ and A are the bulk fluid outlet temperature, bulk fluid inlet temperature and inner surface area of the copper pipe. The Nusselt number (Nu) then can be calculated as (Eq. (10)):

$$Nu(x) = \frac{h(x)\, D_i}{k} \quad (10)$$

where, D_i and k are the inside diameter of the copper tube and the thermal conductivity of the test fluid respectively.

3. Results and discussion

3.1. TEM and XRD analysis

In order to examine the morphology of rutile TiO_2 used in this study, transmission electron microscopy (TEM) analysis of TiO_2 nanoparticles was done. Fig. 2 depicts the TEM image of the TiO_2 nanoparticles. The TiO_2 nanoparticles are having spherical morphology with average particles size of less than 100 nm without

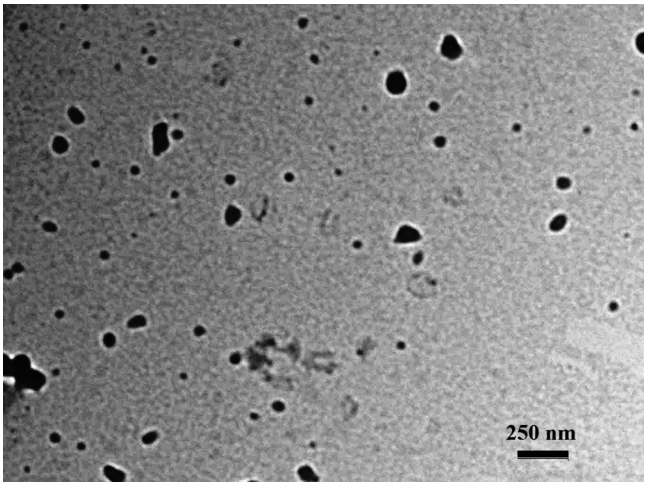

Fig. 2. Transmission Electron Microscopy (TEM) image of TiO_2 nanoparticles used in heat transfer enhancement studies using nanofluids.

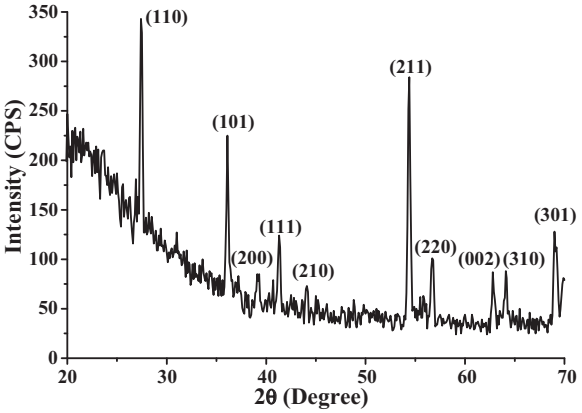

Fig. 3. X-ray diffraction pattern of rutile TiO_2 nanoparticles.

any agglomeration. Dispersion of TiO_2 nanoparticles in basefluid has been effectively achieved with the use of ultrasonic irradiation, which avoids the agglomeration. The average particle size of TiO_2 nanoparticles in the nanofluid suspension is also confirmed by particle size analysis with the use of Malvern Zetasizer Instrument and it was found around 110 nm. XRD pattern of nano-TiO_2 in rutile phase is shown in Fig. 3. XRD pattern exhibited strong diffraction peaks at 27.4, 36.1 and 54.4° corresponding to the planes (1 1 0), (1 0 1) and (2 1 1) respectively indicating TiO_2 in the rutile phase. All peaks are in good agreement with the standard spectrum (JCPDS no.: 88-1175). These results also suggest that the TiO_2 nanoparticles are in crystalline nature.

3.2. Validation of experimental set up

In order to ensure the reliability and accuracy of the fabricated experimental set up, systematic measurements were carried out using deionized water as the working fluid. The experimental results obtained were correlated with well-known Shah correlation [42] under the constant heat flux condition. The equations involved in Shah correlation are:

$$Nu = 1.953\left(Re \cdot Pr\frac{D_i}{x}\right)^{1/3} \quad \text{if } \left(Re.Pr\frac{D_i}{x} \geq 33.3\right) \tag{11}$$

$$Nu = 4.364 + 0.0722\left(Re \cdot Pr\frac{D_i}{x}\right) \quad \text{if } \left(Re.Pr\frac{D_i}{x} \leq 33.3\right) \tag{12}$$

where, *Nu* is the Nusselt number, *Re* is the Reynolds number and *Pr* is the Prandtl number. The experimental values were reasonably in good agreement with the Shah equation, which is reported in Fig. 4. The RMSE value calculated for Shah model's predictions was found to be 1.65. A good coincidence between the experimental results and the calculated values for water reveals the precision of the experimental system, which is considerably good.

3.3. Effect of composition of basefluid on heat transfer

In this work, experiments were carried out to estimate the heat transfer coefficient of basefluid with varying volume percent of EG in water from 10 to 50%. Fig. 5 shows the Nusselt number as a function of axial position for different volume concentrations of EG at Reynolds number of 1500. It can be found from the result that as the concentration of EG increases the Nusselt number increases. The Nusselt number value increases from 8.25 to 20.52 with an increase in the EG concentration from 0 to 50%. The Nusselt number value at 40% EG concentration is 19.15. This increase in the Nusselt number is attributed to the higher specific heat capacity and viscosity of EG–water mixture which will increase Npr that may increase Nusselt number at same Reynolds number.

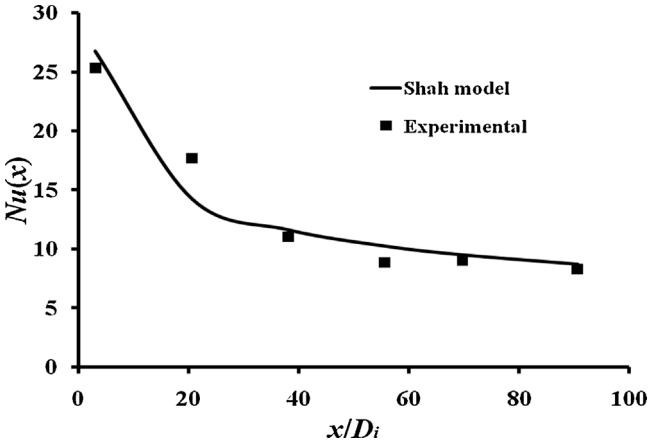

Fig. 4. Validity of experimental heat transfer setup using DI water.

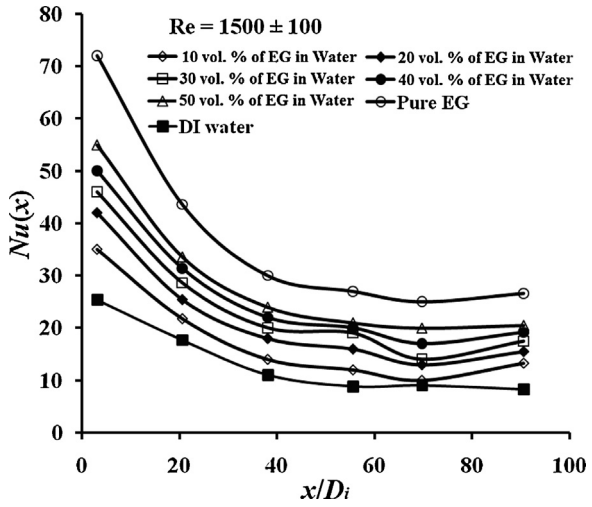

Fig. 5. Effect of volume % of EG in water on Nusselt Number.

Further, thermal conductivity of EG is lower than that of water which can affect the convective heat transfer. It will increase the Nusselt number with an increase in the concentration of EG. Thus considering the heat transfer characteristics and other properties, basefluid with 40% EG and 60% water was selected for further experimentation, which was also reported in the literature [30].

3.4. Effect of volume fraction of TiO_2 nanoparticles on heat transfer of nanofluids

The various studies in the literature have shown that the concentration of nanoparticles enhances the heat transfer coefficient efficiently. Fig. 6 shows the local convective heat transfer coefficients for nanofluids with various volume fractions of TiO_2 nanoparticles (0.1, 0.2, 0.3, 0.4, and 0.5 vol.%) and basefluid at Reynolds number of 1500 ± 50.

The convective heat transfer coefficient is 4734.77 W/m^2 °C at the entrance region and it is significantly higher up to $x/D_i = 20.6$ than that in the other regions (1533.95 W/m^2 °C at $x/D_i = 90.625$) for 0.1 vol.% TiO_2 in nanofluid. It is attributed to entrance effect of nanofluid in the test section. Fig. 7 shows the heat transfer coefficient enhancement due to an increase in the concentrations of TiO_2 nanoparticle in the nanofluids. It can be seen that with an addition of 0.1 vol.% of TiO_2 nanoparticle into the basefluid, there is an increase of heat transfer coefficient about 58% in comparison with the basefluid, which was further enhanced with an increase in

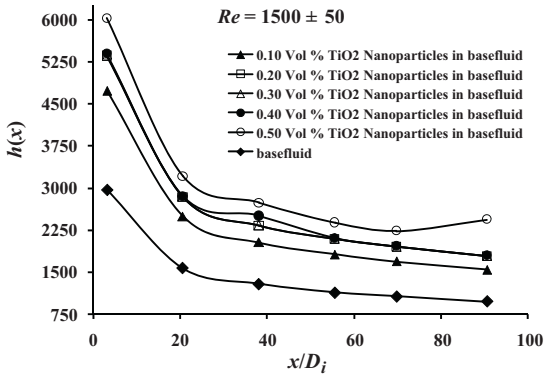

Fig. 6. Axial variation of convective heat transfer co-efficient as a function of TiO_2 nanoparticles concentration in basefluid (40 vol.% EG in water).

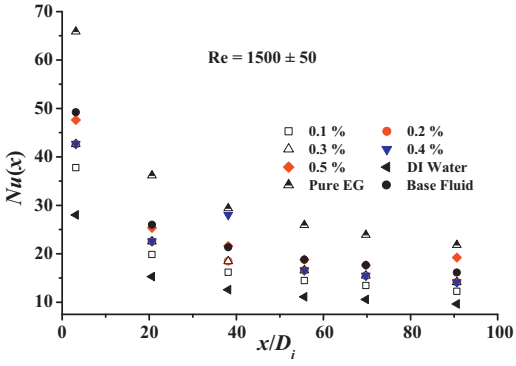

Fig. 8. Axial variation of Nusselt Number of nanofluid as a function of TiO_2 nanoparticles concentration in basefluid (40 vol.% EG in water) at $Re = 1500 \pm 50$.

the nanoparticle concentration. This enhancement in heat transfer coefficient can be explained by following two mechanisms:

(1) Firstly, the addition of the nanoparticles may have actually been instrumental to cause an earlier transition from laminar to turbulent flow which would mean higher heat transfer coefficient value. This enhancement would only be expected to occur within a very narrow region of Reynolds numbers. Once the basefluid transitioned to turbulent flow, similar heat transfer performance would be expected.
(2) A second mechanism which might explain this small enhancement observed lies with the rheology of the fluid. Because the nanofluid is shear-thinning and the shear rate is highest near the wall, better fluid flow performance should be realized near the wall. Further the enhancement is also attributed to reduced drag and hence the pressure drop leading to improvement in the flow behavior of nanofluid.

Further from Fig. 7, 60% enhancement in heat transfer coefficient is observed at 0.1 vol.% loading of TiO_2 nanoparticles in basefluid. For 0.2 to 0.4 vol.% loading of TiO_2 nanoparticle loading an enhancement in heat transfer coefficient is around 84% and at 0.5 vol.% loading of TiO_2 nanoparticles, it is 105%. 0.2–0.4 vol.% TiO_2 nanoparticles loading in nanofluid does not show a monotonous increase in the heat transfer coefficient. It is attributed re-arrangement of TiO_2 nanoparticles in the nanofluid due to non-uniform shear rate.

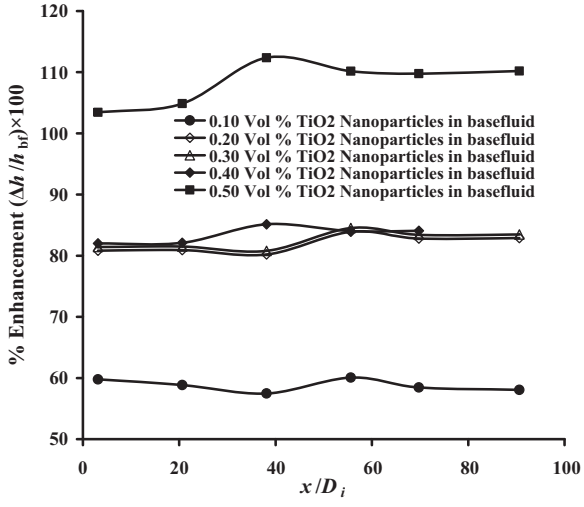

Fig. 7. Axial variation of percentage enhancement in heat transfer coefficient of nanofluid at $Re = 1500 \pm 50$ as a function of TiO_2 nanoparticles concentration in basefluid (40 vol.% EG in water).

The viscosity and thermal conductivity of TiO_2 nanofluids decreases with shear rate, and increases with temperature, respectively. These may lead to a non-uniform viscosity and thermal conductivity enhancement due to re-arrangement of TiO_2 nanoparticles in the nanofluid i.e. non-uniform distribution of TiO_2 nanoparticles in the nanofluid [39].

The inclusion of TiO_2 nanoparticles can significantly enhance the convective heat transfer coefficient, which increases with increasing particle concentrations. The heat transfer coefficient is generally represented as $k/\delta t$ where k and δ_t are the thermal conductivity of the nanofluid and the thickness of the thermal boundary layer, respectively. An increase in k and the decrease in δ_t lead to increase in the value of heat transfer coefficient. Further, this is generally described by a probable boundary layer thinning effect which is caused by the presence of TiO_2 in the nanofluid. Apart from the improved effective thermal conductivity the improvement in the heat transfer is also attributed to particle migration, which caused a non-uniform distribution of thermal conductivity and viscosity field along the tube cross-section (and/or the possibility of a reduced boundary layer) [14]. Further an increase in the volume fraction of the nanoparticles enhances the interaction and collision of the nanoparticles and also the diffusion and relative movement of these particles near the walls lead to faster heat transfer from the walls to the nanofluid. This increase in the volume fraction of the nanoparticles also changes the pressure drop, thermal conductivity, viscosity etc.

The experimental results of for pure water, pure EG, basefluid and the nanofluid containing TiO_2 nanoparticles ranging from 0.1 to 0.5 vol.% under the same flow conditions are shown in Fig. 8. On comparison the Nusselt number of nanofluids is found to be higher than the water, the observed improvement in the Nusselt number value is 35% with the addition of 0.1% of the nanoparticles.

When compared to basefluid it shows that for the nanofluids with up to 0.4 vol.% TiO_2, the Nusselt number is lower than that of basefluid and further it is increased for 0.5 vol.% TiO_2. The figure also depicts that pure EG has the maximum Nusselt number, but for the practical situations the use of pure EG may lead to very high-pressure drop and viscous flow conditions. The nanofluid shows the higher Nusselt number only above 0.5 vol.% of the TiO_2 concentration. So the nanofluid with the 0.5 vol.% TiO_2 concentration is considered for further investigations of the effect of inlet temperature and the nanofluid flow rate on heat transfer performance. Further the addition of surfactant to nanofluid causes no noteworthy change in physical properties, except viscosity and surface tension. The addition of small amount of surfactant additives can also reduce the solution's surface tension significantly, and its level of reduction depends on the amount and type of surfactant presented in the solution [43]. Further, the major effect of surfactant gives change in surface tension and no impact on heat transfer.

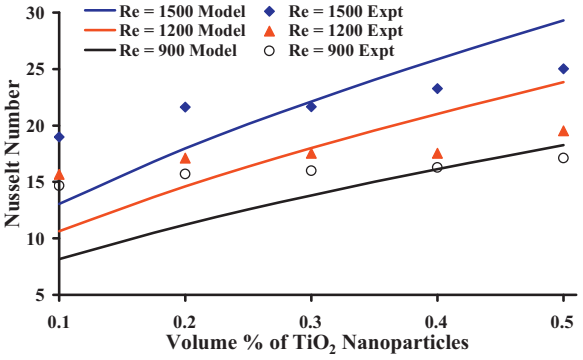

Fig. 9. Comparison of experimental results for Nusselt Number of nanofluid as a function of TiO_2 nanoparticles concentration in nanofluid and predictions of Xuan and Li [43] empirical correlations for laminar flow of the nanofluids in tube.

Fig. 9 reports comparison of experimental results for Nusselt Number of nanofluid as a function as TiO_2 nanoparticles concentration in nanofluid and predictions of Xuan and Li [44] empirical correlations (Eq. (13)) for laminar flow of the nanofluids in tube.

$$Nu = 0.0059(1 + 7.6286\varphi^{0.6886}Pe^{0.001})Re^{0.9238} \quad Re < 2100 \qquad (13)$$

The experimental data obtained in the present investigation have been compared with the correlation given in Eq. (13). The experimental results given in Fig. 9 for the Nusselt number of TiO_2/water–EG nanofluids shows good agreement with the prediction of Xuan and Li [44] correlation. Further calculating the root mean square errors (RMSE) reveals that the RMSE for Reynolds number 1500 is 3.8 whereas it is 3.5 and 3.7 for Reynolds number 1200 and 900 respectively.

3.5. Effect of inlet temperature on heat transfer of nanofluids

In case of nanofluids, the change of inlet temperature affects the Brownian motion of nanoparticles and clustering of nanoparticles [40], which results in dramatic changes in thermal conductivity of nanofluids with temperature. Fig. 10 compares Nusselt numbers of the nanofluid at different inlet temperatures in order to analyze the effect of temperature variation on the heat transfer performance of the nanofluids. It is clear that with an increase in the nanofluid inlet temperature from 30 to 60 °C there is an improvement in the heat transfer performance. This variation in Nusselt number may be attributed to the effect of temperature on Brownian motion of nanoparticles and clustering of nanoparticles which might have increased the thermal conductivity of the nanofluid.

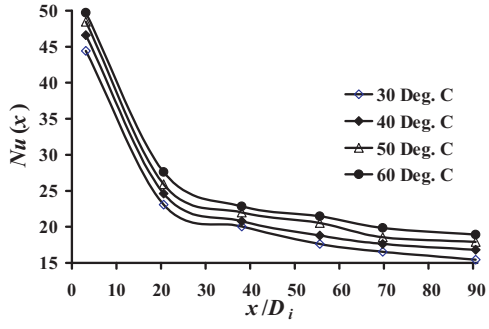

Fig. 10. Effect of inlet temperature on Nusselt Number of nanofluid for 0.5 vol.% of TiO_2 nanoparticles concentration in basefluid (40 vol.% EG in water) at $Re = 1500 \pm 50$.

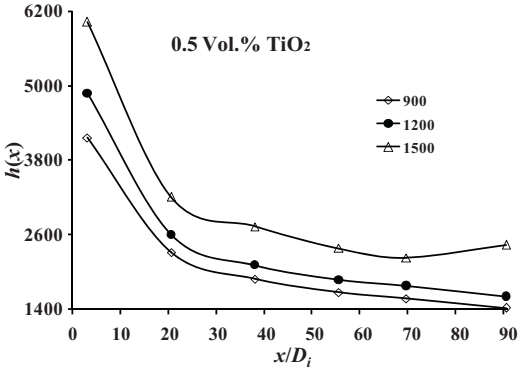

Fig. 11. Axial variation of convective heat transfer co-efficient of nanofluid for 0.5 vol.% of TiO_2 nanoparticles concentration in basefluid (40 vol.% EG in water) with Reynolds Number.

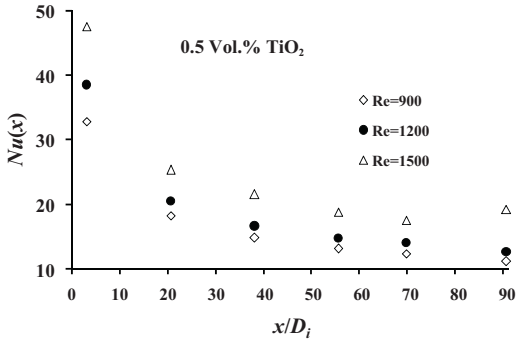

Fig. 12. Axial variation of Nusselt number of nanofluid for 0.5 vol.% of TiO_2 nanoparticles concentration in basefluid (40 vol.% EG in water) with Reynolds Number.

3.6. Effect of flow rate on heat transfer of nanofluids

It is well known that the flow characteristics of the fluid affect the convective heat transfer to a greater extent. Increased flow rate induces eddies in the flow, which ultimately help in increasing the heat transfer. Fig. 11 shows the variation of the convective heat transfer coefficient of 0.5 vol.% TiO_2 nanofluid sample with respect to non-dimensioned axial distance (x/D_i) for different Reynolds number. It can be seen that the laminar heat transfer coefficient decreases with axial distance, which may be due to increased viscosity, thermal conductivity and specific heat of the nanofluid. For a pure Newtonian fluid flowing through a tube with a circular cross section, the flow is considered to be fully developed hydrodynamically and thermally at $x/D_i \geq 0.05Re$ and $x/D_i \geq 0.05.RePr$, respectively. It can be seen from the figure that, once the flow becomes fully developed, the heat transfer coefficient value stabilizes for nanofluids. A significant enhancement in heat transfer coefficient was observed as the Reynolds number gets increased from 900 to 1500. Further the Nusselt number for the constant diameter increases with an increase in the Reynolds number and is reported in Fig. 12. At low Reynolds number, an agglomeration of nanoparticles might be possible in the nanofluid flow. This will lead to lower heat transfer enhancement at lower Reynolds number. However, at high Reynolds number, the agglomeration effect is significantly reduced and dispersion of the nanoparticles intensifies the mixing, which results in significant increase in the heat-transfer coefficient.

4. Conclusions

In this work, the convective heat transfer performance of EG–water based nanofluids in copper tube has been investigated.

The particle size of TiO_2 nanoparticles used was less than 100 nm which was confirmed from TEM analysis. It can be concluded that with an increase in the concentration of EG the Nusselt number increases. Significant increases in the heat transfer coefficient (105% for 0.5 vol.% of TiO_2 nanoparticles) have been observed with the TiO_2 nanoparticle addition. Performance of nanofluid when compared with deionized water, there was 60% enhancement in the heat transfer coefficient for 0.1 vol.% of TiO_2 nanoparticles in the basefluid. The maximum percentage enhancement in heat transfer coefficient was 105% at $Re = 1500 \pm 50$ for 0.5 vol.% of TiO_2 nanoparticles in the nanofluid. It is also found that with an increase in the fluid inlet temperature (30–60 °C) significantly increases the Nusselt number value which can be attributed to the effect of temperature on the physical properties. Further the Nusselt number was found to increase with an increase in the Reynolds number. It is attributed to the reduction of agglomeration effect and intensification of mixing due to the dispersion of the nanoparticles. Thus improving the heat transfer characteristics and compatibility of TiO_2 nanofluid based on EG–water mixture can be a great option in heat transfer equipments.

Acknowledgements

B.A. Bhanvase is thankful to Prof. A. B. Pandit, Institute of Chemical Technology, Mumbai for his valuable guidance to carry out this work. Authors are also thankful to Vishwakarma Institute of Technology, Pune for providing the facility for this work.

Appendix-I.

- Volumetric flow rate of nanofluid = 3.17×10^{-5} m/s
- Cross sectional area copper tube = 5.03×10^{-5} m^2
- Mass flow rate nanofluid = 0.03322 kg/s
- Velocity of nanofluid = 0.63 m/s
- Inner diameter of copper tube = 0.008 m
- Specific heat (C_P) of nanofluid from Eq. (2) = 3385.416 J/kg. °C
- Density of nanofluid from the Eq. (3) = 1049.15 kg/m^3
- Thermal conductivity of nanofluid from the Eq. (4) = 1.002573 W/m. °C
- Viscosity of nanofluid from the Eq. (5) = 0.0044 Pa s
- Perimeter = 0.025 m
- Volume fraction of TiO_2 nanoparticles in nanofluid = 0.001
- Reynolds number $Re = \frac{DV\rho}{\mu} = 1201.1$
- Prandtl number $Pr = \frac{C_P\mu}{k} = 14.86$
- Themal diffusivity $\alpha = \frac{k}{\rho C_P} = 2.82 \times 10^{-7}$ m^2/s
- Heat flux q_s from the Eq. (9) = 5370.129 W/m^2
- Bulk temperature of the nanofluid ($T_b(x)$) at an axial distance, x is calculated using Eq. (8) and it is equal to 30. 86 °C at $x/D_i = 90.625$
- Convective heat transfer coefficient $h(x)$ at an axial distance 'x' from the inlet is calculated using Eq. (7) and it is equal to 1298.822 W/m^2 °C at $x/D_i = 90.625$
- Nusselt number is estimated using Eq. (10) and it is equal to 10.364 at $x/D_i = 90.625$

References

[1] S.U.S. Choi, Enhancing thermal conductivity of fluids with nanoparticles, in: D.A. Siginer, H.P. Wang (Eds.), Developments Applications of Non-Newtonian Flows, FED-vol. 231/MD-vol. 66, ASME, New York, 1995, pp. 99–105.
[2] H. Masuda, A. Ebata, K. Teramae, N. Hishiunma, Alteration of thermal conductivity and viscosity of liquid by dispersed by ultra-fine particles (dispersion of (-Al_2O_3 SiO_2 and TiO_2 ultra-fine particles), Netsu Bussei (Japan) 4 (1993) 227–233.
[3] S.D. Park, S.W. Lee, S. Kang, S.M. Kim, H. Seo, I.C. Bang, Effects of Al_2O_3/R-123 nanofluids containing $C_{19}H_{40}$ core-shell phase change materials on critical heat flux, Int. J. Heat Mass Transfer 55 (2012) 7144–7150.
[4] S. Krishnamurthy, P. Bhattacharya, P.E. Phelan, R.S. Prasher, Enhanced mass transport in nanofluids, Nano Lett. 6 (2006) 419–423.
[5] D.T. Wasan, A.D. Nikolov, Spreading of nanofluids on solids, Nature 423 (2003) 156–159.
[6] X.Q. Wang, A.S. Mujumdar, Heat transfer characteristics of nanofluids: a review, Int. J. Thermal Sci. 46 (2007) 1–19.
[7] W. Duangthongsuk, S. Wongwises, A critical review of convective heat transfer of nanofluids, Renew. Sustain. Energ. Rev. 11 (2007) 797–817.
[8] Y. He, Y. Jin, H. Chen, Y. Ding, D. Cang, H. Lu, Heat transfer and flow behaviour of aqueous suspensions of TiO_2 nanoparticles (nanofluids) flowing upward through a vertical pipe, Int. J. Heat Mass Transfer 50 (2007) 2272–2281.
[9] C.T. Nguyen, G. Roy, C. Gauthier, N. Galanis, Heat transfer enhancement using Al_2O_3–water nanofluid for electronic liquid cooling system, Appl. Thermal Eng. 27 (2007) 1501–1506.
[10] W. Duangthongsuk, S. Wongwises, Heat transfer enhancement and pressure drop characteristics of TiO_2–water nanofluid in a double-tube counter flow heat exchanger, Int. J. Heat Mass Transfer 52 (2009) 2059–2067.
[11] S.M. Peyghambarzadeh, S.H. Hashemabadi, M. Seifi Jamnani, S.M. Hoseini, Improving the cooling performance of automobile radiator with Al_2O_3/water nanofluid, Appl. Thermal Eng. 31 (2011) 1833–1838.
[12] W. Duangthongsuk, S. Wongwises, An experimental study on the heat transfer performance and pressure drop of TiO_2–water nanofluids flowing under a turbulent flow regime, Int. J. Heat Mass Transfer 53 (2010) 334–344.
[13] P. Naphon, P. Assadamongkol, T. Borirak, Experimental investigation of titanium nanofluids on the heat pipe thermal efficiency, Int. Commun. Heat Mass Transfer 35 (2008) 1316–1319.
[14] D. Wen, Y. Ding, Experimental investigation into convective heat transfer of nanofluids at the entrance region under laminar flow conditions, Int. J. Heat Mass Transfer 47 (2004) 5181–5188.
[15] D. Wen, Y. Ding, Formulation of nanofluids for natural convective heat transfer applications, Int. J. Heat Fluid Flow 26 (2005) 855–864.
[16] J.A. Eastman, S.R. Phillpot, S.U.S. Choi, P. Keblinski, Thermal transport in nanofluids, Annu. Rev. Mater. Sci. 34 (2004) 219–246.
[17] S.P. Jang, S.U.S. Choi, Role of Brownian motion in the enhanced thermal conductivity of nanofluids, Appl. Phys. Lett. 84 (2004) 4316–4318.
[18] W. Yu, D.M. France, J.L. Routbort, S.U.S. Choi, Review and comparison of nanofluid thermal conductivity and heat transfer enhancements, Heat Transfer Eng. 29 (2008) 432–460.
[19] P. Bhattacharya, S.K. Saha, A. Yadav, P.E. Phelan, R.S. Prasher, Brownian dynamics simulation to determine the effective thermal conductivity of nanofluids, J. Appl. Phys. 95 (2004) 6492–6494.
[20] H. Xie, J. Wang, T. Xi, Y. Liu, F. Ai, Dependence of the thermal conductivity of nanoparticles-fluid mixture on the base fluid, J. Mater. Sci. Lett. 21 (2002) 1469–1471.
[21] H. Xie, J. Wang, T. Xi, Y. Liu, Thermal conductivity of suspensions containing nanosized SiC particles, Int. J. Thermophys. 23 (2002) 571–580.
[22] C. Pang, J.Y. Jung, Y.T. Kang, Thermal conductivity enhancement of Al_2O_3 nanofluids based on the mixtures of aqueous NaCl solution and CH_3OH, Int. J. Heat Mass Transfer 56 (2013) 94–100.
[23] K.G.K. Sarojini, S.V. Manoj, P.K. Singh, T. Pradeep, S.K. Das, Electrical conductivity of ceramic and metallic nanofluids, Colloids Surfaces A: Physicochem. Eng. Aspects 417 (2013) 39–46.
[24] C. Pang, J.Y. Jung, J.W. Lee, Y.T. Kang, Thermal conductivity measurement of methanol-based nanofluids with Al_2O_3 and SiO_2 nanoparticles, Int. J. Heat Mass Transfer 55 (2012) 5597–5602.
[25] B. Pak, Y. Cho, Hydrodynamic and heat transfer study of dispersed fluids with submicron metallic oxide particles, Exp. Heat Transfer 11 (1998) 151–170.
[26] S.U.S. Choi, Z.G. Zhang, W. Yu, F.E. Lockwood, E.A. Grulke, Anomalous thermal conductivity enhancement in nanotube suspensions, Appl. Phys. Lett. 79 (2001) 2252–2254.
[27] P. Keblinski, S.R. Phillpot, S.U.S. Choi, J.A. Eastman, Mechanisms of heat flow in suspensions of nano-sized particles (nanofluids), Int. J. Heat Mass Transfer 45 (2002) 855–863.
[28] S.K. Das, N. Putra, P. Thiesen, W. Roetzel, Temperature dependence of thermal conductivity enhancement of nanofluids, J. Heat Transfer 125 (2003) 567–574.
[29] X. Wang, X. Xu, S.U.S. Choi, Thermal conductivity of nanoparticle fluid mixture, J. Thermophys. Heat Transfer 13 (1999) 474–480.
[30] M.M. Sarafraz, S.M. Peyghambarzadeh, Influence of thermodynamic models on the prediction of pool boiling heat transfer coefficient of dilute binary mixtures, Int. Commun. Heat Mass Transfer 39 (2012) 1303–1310.
[31] S.M. Peyghambarzadeh, S.H. Hashemabadi, S.M. Hoseini, M. Seifi Jamnani, Experimental study of heat transfer enhancement using water/ethylene glycol based nanofluids as a new coolant for car radiators, Int. Commun. Heat Mass Transfer 38 (2011) 1283–1290.
[32] H. Xie, J. Wang, T. Xi, F. Ai, Q. Wu, Thermal conductivity enhancement of suspensions containing nanosized alumina particles, J. Appl. Phys. 91 (2002) 4568–4572.
[33] S. Lee, S.U.S. Choi, S. Li, J.A. Eastman, Measuring thermal conductivity of fluids containing oxide nanoparticles, J. Heat Transfer 121 (1999) 280–289.
[34] Y. Xuan, Q. Li, Heat transfer enhancement of nanofluids, Int. J. Heat Fluid Flow 21 (2000) 58–64.
[35] S.K. Das, N. Putra, W. Roetzel, Pool boiling of nano-fluids on horizontal narrow tubes, Int. J. Multiphase Flow 29 (2003) 1237–1247.
[36] S.M.S. Murshed, K.C. Leong, C. Yang, Enhanced thermal conductivity of TiO_2–water based nanofluids, Int. J. Thermal Sci. 44 (2005) 367–373.

[37] H. Demir, A.S. Dalkilic, N.A. Kürekci, W. Duangthongsuk, S. Wongwises, Numerical investigation on the single phase forced convection heat transfer characteristics of TiO_2 nanofluids in a double-tube counter flow heat exchanger, Int. Commun. Heat Mass Transfer 38 (2011) 218–228.
[38] A. Turgut, I. Tavman, M. Chirtoc, H.P. Schuchmann, C. Sauter, S. Tavman, Thermal conductivity and viscosity measurements of water-based TiO_2 nanofluids, Int. J. Thermophys. 30 (2009) 1213–1226.
[39] P. Garg, J.L. Alvarado, C. Marsh, T.A. Carlson, D.A. Kessler, K. Annamalai, An experimental study on the effect of ultrasonication on viscosity and heat transfer performance of multi-wall carbon nanotube-based aqueous nanofluids, Int. J. Heat Mass Transfer 52 (2009) 5090–5101.
[40] R. Prasher, W. Evans, P. Meakin, J. Fish, P. Phelan, P. Keblinsk, Effect of aggregation on thermal conduction in colloidal nanofluids, Appl. Phys. Lett. 89 (2006) 143119–1143119.
[41] J.C. Maxwell, Treatise on Electricity and Magnetism, 3rd ed., Oxford University Press, London, 1904.
[42] R.K. Shah, Thermal Entry Length Solutions for the Circular Tube and Parallel Plates, in: Proceedings of the 3rd National Heat Mass Transfer Conference, Indian Institute of Technology, Bombay, 1975.
[43] W. Lu, G.K. Poon, P.L. Carmichael, R.B. Cole, Analysis of tamoxifen and its metabolites by on-line capillary electrophoresis–electrospray ionization mass spectrometry employing nonaqueous media containing surfactants, Anal. Chem. 68 (1996) 668–674.
[44] Y. Xuan, Q. Li, Investigation on convective heat transfer and flow features of nanofluids, J. Heat Transfer 125 (2003) 151–155.